2022

Comparison of stationary and mobile canopy sensing systems for irrigation management of maize and soybean in Nebraska

Sandeep Bhatti
University of Nebraska-Lincoln, sandeep.bhatti@huskers.unl.edu

Derek M. Heeren
University of Nebraska-Lincoln, derek.heeren@unl.edu

Susan A. O'Shaughnessy
USDA-ARS Conservation and Production Research Laboratory, Bushland, Texas, susan.oshaughnessy@usda.gov

Steven R. Evett
USDA-ARS Conservation and Production Research Laboratory, Bushland, Texas, steve.evett@usda.gov

Mitchell S Maguire
University of Nebraska - Lincoln, mmaguire2@unl.edu

See next page for additional authors

COMPARISON OF STATIONARY AND MOBILE CANOPY SENSING SYSTEMS FOR MAIZE AND SOYBEAN IN NEBRASKA, USA

Sandeep Bhatti[1], Derek M. Heeren[1,*], Susan A. O'Shaughnessy[2], Steven R. Evett[2], Mitchell S. Maguire[1,3], Suresh P. Kashyap[1], Christopher M. U. Neale[3,1]

[1] Biological Systems Engineering, University of Nebraska-Lincoln, Lincoln, Nebraska, USA.
[2] USDA-ARS Conservation and Production Research Laboratory, Bushland, Texas, USA.
[3] Daugherty Water for Food Global Institute, University of Nebraska, Lincoln, Nebraska, USA.
[*] Correspondence: derek.heeren@unl.edu

HIGHLIGHTS

- Multispectral sensors mounted on the center pivot lateral were able to capture differences between rainfed and irrigated crop.
- Canopy temperature was strongly associated among stationary and pivot-mounted sensors with coefficient of determination ranging between 0.88 and 0.99.
- A cooling effect of about 2°C was observed in canopy temperature data collected from pivot mounted sensors for irrigated soybean crop.

ABSTRACT. *Accurate knowledge of plant and field characteristics is crucial for irrigation management. Irrigation can potentially be better managed by utilizing data collected from various sensors installed on different platforms. The accuracy and repeatability of each data source are important considerations when selecting a sensing system suitable for irrigation management. The objective of this study was to compare data from multispectral (red and near-infrared bands) and thermal (long wave thermal infrared band) sensors mounted on different platforms to investigate their comparative usability and accuracy. The different sensor platforms included stationary posts fixed on the ground, the lateral of a center pivot irrigation system, unmanned aircraft systems (UAS), and Planet (PlanetScope multispectral imager, Planet Labs, Inc., San Francisco, Calif.) satellites. The surface reflectance data from multispectral (MS) sensors were used to compute the Normalized Difference Vegetation Index (NDVI) and Soil Adjusted Vegetation Index (SAVI). The experimental plots were managed with rainfed and irrigated treatments. Irrigation was applied according to a spatial evapotranspiration model informed with Planet satellite imagery. The NDVI and SAVI curves computed from the different sensing systems exhibited similar patterns and were able to capture differences between the rainfed and irrigated treatments when the crops were approaching senescence. Strong correlations were observed for canopy temperature measurements between the stationary and pivot-mounted infrared thermometer (IRT) sensors (p-value of less than 0.01 for the correlations) when canopy were scanned with no irrigation application (dry scans). The best correlation was obtained for the irrigated maize, which yielded r^2 of 0.99, RMSE of 0.4°C, and MAE of 0.3°C. The correlation for the canopy temperature data collected during dry scan between UAS and pivot-mounted thermal sensors was weak with r^2 = 0.26 to 0.28, larger RMSE values of 3.7°C and MAE values of 3.4°C. Secondary analysis between thermal data from stationary and pivot-mounted IRTs collected during wet scans (during an irrigation event) demonstrated reduced canopy temperature from pivot-mounted IRTs by approximately 2°C for irrigated soybean due to wetting of the canopy by the irrigation. Understanding the performance of these sensor systems is valuable in configuring practical design and operational considerations when using sensor feedback for irrigation management.*

Keywords. *Center pivots, Irrigation, Multispectral, Remote sensing, Thermal, Unmanned aircraft systems.*

Remote and proximal sensing can be important to acquiring data essential for precision agriculture. Precision agriculture constitutes the management of a field at a sub-field scale by applying management that changes in space and time, which may require division of the field into management zones (Zhang et al., 2002; Daccache et al., 2015). The management zones should be continuously monitored by collecting spatiotemporal data using various sensing systems (Evans et al., 2013;

Submitted for review on 4 November 2021 as manuscript number NRES 14945; approved for publication as a Research Article by the Natural Resources & Environmental Systems Community of ASABE on 27 January 2022.

Mention of company or trade names is for description only and does not imply endorsement by the USDA. The USDA is an equal opportunity provider and employer.

Higgins et al., 2016; Miller et al., 2018). These systems include sensors, sensor network systems, and the platforms used to mount or move the sensors. Sensors may include soil water sensors, MS sensors, or thermal sensors (infrared thermometers and imagers), with the aim being to manage and avoid excessive water-related stress in the crop (Osroosh et al., 2016). The sensors used for irrigation management are mainly focused on maintaining appropriate levels of soil water in the root zone. However, the soil water-based irrigation methods do not account for physiological characteristics of the crop and atmospheric aridity. The irrigation methods including components of crop physiological characteristics, atmospheric aridity, and soil water availability, are important for sustainable irrigation schemes (Zhang et al., 2021). Therefore, soil water sensing should be used in conjunction with remote sensing of the crop canopy and weather data to better inform irrigation decisions.

Sensor platforms could be either stationary or mobile and ground-based or aerial-based (Taghvaeian et al., 2020). It is common to install sensors at fixed locations in a research field using stationary posts. These fixed sensing systems are easy to install and provide a fine time-scale temporal trend of sensed data (Evett et al., 1996). However, the stationary systems can only capture characteristics of a limited area (~0.1 m^2; DeJonge et al., 2015), which is less than optimal for site-specific management of large-scale fields. In contrast, sensors mounted on moving platforms are capable of collecting spatial data with fewer sensors but without a continuous time-scale data record at any one point in space, which could be crucial for water management. Common moving sensor platforms include aerial systems or any ground-based moving equipment. Aerial systems, such as UAS and satellites, have been widely used as moving platforms for sensors that can inform remote sensing-based models for irrigation management (Cohen et al., 2015; Kim et al., 2018; Quebrajo et al., 2018; Barker et al., 2019; Bhatti et al., 2020; Ohana-Levi et al., 2020). An example is the Spatial Evapotranspiration Modeling Interface (SETMI; Geli and Neale, 2012; Neale et al., 2012), a remote sensing-based model capable of informing irrigation decisions using imagery from different aerial systems. Energy balance models such as Soil Energy Balance for Land (SEBAL; Bastiaanssen et al., 1998), the Mapping EvapoTranspiration at high Resolution with Internalized Calibration (METRIC; Allen et al., 2007), and High Resolution Mapping of Evapo-Transpiration (HRMET; Zipper and Loheide, 2014), are widely used to estimate evapotranspiration using remote sensing imagery. However, aerial and spaceborne systems may induce inaccuracies in sensor data due to atmospheric interference and sensor heating (Maguire et al., 2021).

Ground-based moving platforms are a viable option for proximal sensing of crop canopy parameters including canopy temperature, NDVI, leaf area index, and fraction of cover. Center pivot irrigation systems and linear-move systems cover a large portion of the irrigated acreage in the U.S. (Evans et al., 2013; O'Shaughnessy et al., 2016; Evett et al., 2020). IRT sensors and other imagers have been mounted on center pivot and linear-move irrigation systems to study different crop parameters and crop water stress (O'Shaughnessy et al., 2013; Colaizzi et al., 2019; Sui et al., 2020). Center pivots are primarily designed to distribute water across the field to meet crop water needs. However, center pivots could also be used to mount sensors to estimate canopy cover, crop health, and soil interference (Evett et al., 2020). Further, multispectral sensors mounted on the pivot can provide valuable spatial information on crop health and fraction of cover by estimating various vegetation indices (VIs). The two common VIs in agriculture are NDVI (Normalized Difference Vegetation Index; Rouse et al., 1973) and Soil Adjusted Vegetation Index (SAVI; Huete, 1988), which are useful for estimation of evapotranspiration and irrigation requirements (Campos et al., 2010). These VIs incorporate red and near infrared band reflectance values from the target surface and can be used to examine plant health. In addition to accounting for differences in reflectance among red and near infrared bands, SAVI also includes a correction factor that accounts for the influence of soil brightness. The vegetation indices are not solely used for irrigation management, but are currently used in conjunction with other irrigation methods including soil water balance approach (Taghvaeian et al., 2020). The temporal trend in VI estimated from pivot-mounted MS sensors can detect long term physiological effects from crop water stress on the crop canopy (Zhang et al., 2019), but does not provide the real time information on crop water stress that can be obtained using thermal sensing.

Important features of a successful sensing system for a commercial producer sized field are reliability and scalability (O'Shaughnessy et al., 2013). With current advances in communication and sensor network systems, sensing systems are capable of connecting multiple sensors or nodes for expanding the sensing area of interest (O'Shaughnessy and Evett, 2010). However, it is vital to test the reliability and accuracy of these sensing systems for different watering conditions in a field. While extensive research is being conducted to study and compare sensors in a lab or controlled environment, more research is needed to compare sensors on different platforms and to compare their ability to sense important crop physiological parameters at a management scale typical for an agricultural field. The data from these sensing systems should also have an acceptable accuracy to correctly inform the irrigation models.

This study aimed at comparing different sensors mounted on various platforms in the context of irrigation management for maize and soybean in the sub-humid climate of eastern Nebraska. The objectives of this study were to compare and evaluate the 1) SAVI and NDVI data computed from the pivot, UAS and Planet sensing systems; 2) canopy temperature data from the stationary, pivot, and UAS thermal sensing systems; and 3) irrigation effects on canopy temperature sensed by IRTs mounted on the center pivot.

Materials and Methods

This study was conducted at the University of Nebraska's Eastern Nebraska Research, Extension and Education Center (ENREEC) situated near Mead, Nebraska, during the 2020 growing season. The 58-ha field (centered at 41.172445°N, 96.478248°W; 14T 711538.71 mE, 4560966.1 mN) was

equipped with a center pivot irrigation system, model Valley Irrigation 8000 (Valmont, Valley, Neb.) and fitted with high-speed X-Tec center drive motor. The north and south halves were planted to soybean and maize, respectively. The planting dates were 24 April and 2 May for maize and soybean, respectively. The soils in the field site were primarily classified as silt loam and silty clay loam (gSSURGO, Soil Survey Staff, 2018). The specific soils included Yutan silty clay, Filbert silt loam, Tomek silt loam and Fillmore silt loam.

The field was divided into eight radial zones and 24 arc-wise plot boundaries defining 192 plots, which were managed using rainfed or irrigated methods (fig. 1). The north and south halves had a total of 96 plots each. The plots used in this study were from the outer radial zones and thus were approximately rectangular shaped with an area ranging between 1870 and 2630 m^2. The length of the plots varied between 65 and 90 m. The width of the plots was 28 m. The plots selected for analysis were located in spans 6 and 7 of the center pivot. This study was part of a larger study with a complex experimental design comprised of multiple irrigation treatments. The irrigation scheduling for the plots used in this study was managed by the Spatial EvapoTranspiration Modeling Interface (SETMI; Geli and Neale, 2012; Neale et al., 2012). The rainfed plots received no irrigation during the growing season. A 6.1 m inner buffer around the four edges of each plot was used to remove boundary effects from neighboring plots in data collection and irrigation management.

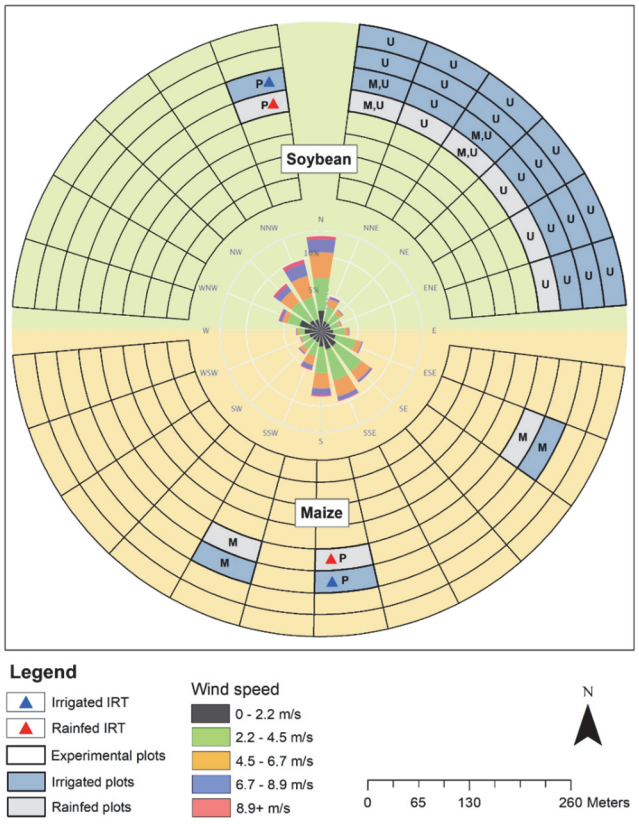

Figure 1. Experimental plots used for the study. The north half shown in light green color was planted to soybean and south half shown in mustard color was planted to maize. The plots with grey color were not irrigated and plots with blue color were irrigated. The plots shown in light green or mustard color were not included in the analyses. The letters 'M', 'P', and 'U' were used to denote type of analysis conducted on a particular plot: M stands for multispectral analysis, P stands for analysis including data from center pivot-mounted IRTs and stationary IRTs, and U stands for analysis including data from center pivot-mounted IRTs and UAS. The windrose diagram shown in the center of the figure was taken from the High Plains Regional Climate Center database. The windrose diagram represents wind from a nearby weather station called Memphis 5N (about 5 km away from the study site) on an annual time scale.

Data Collection

Three different MS sensing systems were used in this study (table 1). Spectral reflectance sensors (SRS; model SRS-NDVI, Meter Group, Inc., Pullman, Wash.) were mounted at a height of 3.6 m at four different locations on span 6 of the pivot lateral (fig. 2). A downlooking SRS was installed on the pivot lateral over the rainfed and irrigated treatments each. Only one uplooking sensor was used for both treatments since the incoming radiant flux was similar for both treatments. The downlooking SRS sensor had a field of view of 36° and was aimed at an angle of about 45° from the horizontal to measure reflected radiation from the target surface in the red (650 ± 10 nm) and near infrared (810 ± 10 nm) bands (area of surface sensed without any canopy cover was approximately 5 m^2). The uplooking sensor had a view angle of 180° and sensed downwelling radiation. These sensors were mounted at distance of about 3 m in the forward/clockwise direction from the sprinklers on the pivot lateral using extension arms (fig. 2). The SRS sensed data at a frequency of five minutes. The data were collected using a model ZL-6 datalogger (Meter Group, Inc., Pullman, Wash.) mounted on the pivot lateral. The center pivot GPS data were used to geolocate the SRS data collected by the datalogger. The data were retrieved from the datalogger using ZENTRA Cloud (Meter Group, Inc., Pullman, Wash.). The second source of MS remote sensing was the PlanetScope MS imager from the Planet satellite (Planet Labs, Inc., San Francisco, Calif.). It captured MS imagery at 3 m spatial resolution and temporal resolution of approximately one day. There were 20 Planet images for maize and 18 Planet images for soybean that were used to inform SETMI for computing the VIs. The MS imagery from Planet were acquired over the field between 10:30 A.M. and 11:30 A.M. The third source was the RedEdge MicaSense camera mounted on the UAS (DJI Matrice 600, Los Angeles, Calif.), which captured imagery at a spatial resolution of 0.08 m. The UAS imagery was acquired at an altitude of approximately 122 m above ground level with imagery collected only over the northeastern quarter of the field planted with soybean. The UAS data were acquired between 11 A.M. and 3 P.M.

Canopy temperature data were taken using three sensing systems (table 1). The first sensing system consisted of IRT sensors (SAPIP-IRT, Dynamax, Inc., Houston, Tex.) mounted on stationary posts. These sensors had a field of view (FOV) of 20° and a spectral range of 5.5 to 14 µm (Colaizzi et al., 2018). For each crop, a single stationary IRT sensor was installed in an irrigated plot and another in a rainfed plot. The IRT sensors on the stationary posts were installed with a nadir view angle. The height of the IRT sensors was adjusted throughout the growing season at least once a month to maintain an approximate height of 1 m above the crop canopy. At full canopy height, the height of the stationary IRT from the

Table 1. Different sensors and corresponding platforms used for data collection.

Sensor	Platform	Data Collected
Spectral reflectance sensors	Pivot lateral	Multispectral
MicaSense	Unmanned aircraft systems	Multispectral
PlanetScope imager	Planet satellite	Multispectral
Dynamax infrared thermometers	Stationary post	Thermal
Dynamax infrared thermometers	Pivot lateral	Thermal
Flir Duo Pro R	Unmanned aircraft systems	Thermal

soil surface was about 3 m for maize and about 2.2 m for soybean. The spacing between the sensor and crop canopy for maize could not be maintained at full canopy height since the sensor post had to be kept below the center pivot. The stationary post was installed in between two rows and the stationary IRT was positioned directly above a crop row.

The second sensing system consisted of four IRT sensors mounted on the center pivot lateral with a pair of IRTs mounted over the rainfed and irrigated plots each. Pivot-mounted IRTs were installed at a spacing of 6.1 m from the edge of the plot borders along the lateral (fig. 2). The height of pivot-mounted sensors was about 3.6 m from the ground surface. The paired IRT sensors were pointed inwards from the opposite sides of a plot toward the center of the plot at an azimuthal angle of about 45°. The IRTs were also adjusted at an oblique angle downward from the horizontal to maximize viewing of vegetation and minimize soil background effects (Colaizzi et al., 2019). Similar to pivot-mounted SRS, IRTs on the pivot were also installed about 3 m ahead of the pivot lateral in the forward/clockwise direction of travel using extension arms (fig. 2). The pivot sensors were mounted in forward direction to minimize the interference of water from the sprinklers during an irrigation event on the sensor reporting. Data taken from both paired IRTs over a management zone were averaged at every timestamp to reduce the effects of the changing sun angle with respect to the view angles of the moving pivot-mounted IRTs. The IRTs sensed canopy temperature with a frequency of five seconds and averaged readings over 1 min. The wireless IRT sensing system involved transmission of sensor data through a coordinator (model SAP-IP-Coordinator, Dynamax, Houston, Tex.), which passed data on to an embedded computer installed at the pivot point, which was used to collect, georeference, timestamp, and store the data from the IRTs.

The UAS imagery included thermal infrared data collected using a FLIR Duo Pro R (Flir Systems Inc., Wilsonville, Ore.), which captured imagery at a spatial resolution of 0.15 m. The UAS data were acquired between 11 A.M. and 3 P.M. with a flight duration of about 17 min and altitude of approximately 122 m. The procedure used to acquire thermal UAS data was similar to Maguire et al. (2021) and more details about data collection and processing can be found in Kashyap (2021). The thermal camera was warmed up at least for an hour before the data collection. During the flight, flat field corrections were performed periodically to compensate for different errors produced by the thermal camera. These corrections were used to re-calibrate the sensor array by accounting for changes in camera body temperature and individual pixel drift (Maguire et al., 2021). Thermal imagery data were not corrected for atmospheric interference. The thermal imagery taken from an adjacent field (south of the study site) with similar soils using the same systems and same altitude were applied with atmospheric corrections (Maguire et al., 2021). It was found that the corrected data were similar to the raw thermal data. As discussed earlier, thermal infrared imagery was only collected for the northeastern quarter of the field, which was in soybean. The aerial imagery allowed spatial patterns in thermal imagery of the crop canopy to be characterized at a finer scale.

Irrigation Management

Irrigation was managed using the SETMI model with satellite imagery from Planet Labs. Satellite imagery with cloud cover near the field area was not used in the model. The water balance component of the model was used along with

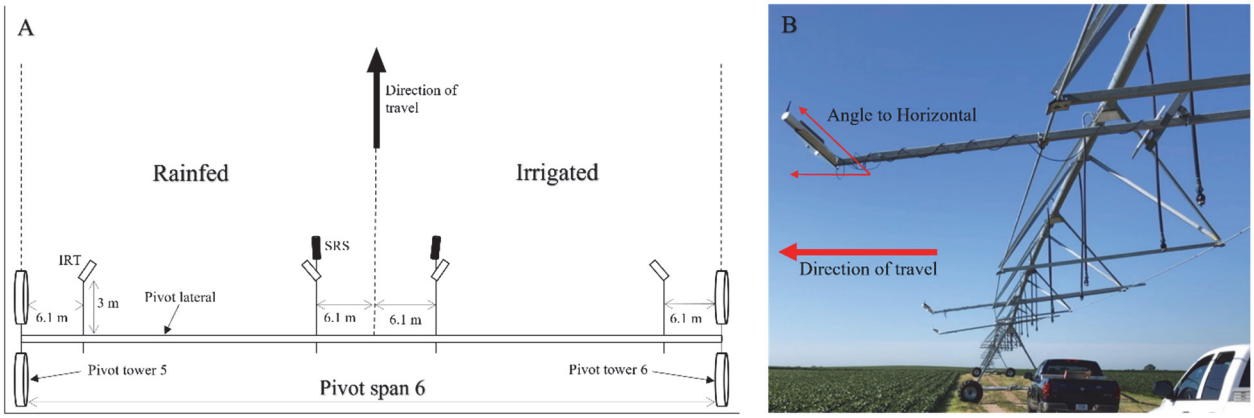

Figure 2. Orientation of sensors mounted on the pivot with A) top view and B) side view. The top view shows rainfed and irrigated plots in span 6 of the pivot. The 6.1 m buffer around the edges of rainfed and irrigated plots is also shown in the top view. Two IRT sensors and one SRS were used for each management zone. The 'Angle to Horizontal' label illustrates the angle at which the sensor was mounted from the horizontal. The SRS and IRT sensors were positioned such that their corresponding field of view was directed towards the center of the plot. The tilt of the pivot structure was also observed due to weight of the mounting equipment.

occasional updates from soil water data from the neutron probe, model 503 Elite Hydroprobe (CPN, Concord, Calif.). The field calibration from a nearby field (within 3 km) with similar soils was used for the neutron probe to obtain volumetric soil water content from neutron count data. The neutron probe was used to acquire soil water data at depths of 15, 45, 76, and 107 cm. The data were taken once every three weeks during the growing season. Soil water data from three locations for each crop were used to update the model. The model had the capability of forecasting irrigation needs based on the historic long term weather data. The model was used in a manner similar to Bhatti et al. (2020), which can be referred to for more details about the irrigation management. The field capacity and wilting point used for this study were 0.40 and 0.20 m^3 m^{-3}, respectively. These values were obtained by averaging estimated field capacity and wilting point measurements in a nearby field (Bhatti et al., 2020) with similar soils.

The sprinklers on the center pivot were spinners model S3030 (Nelson Irrigation, Walla Walla, Wash.) with yellow spray plate installed on drops at a height of 2.4 m from the ground surface and with sprinkler spacing of 2.7 m. The radius of throw (wetted radius) for the sprinklers in the last span was about 7.6 m, which meant that the canopy would be wetted by irrigation within the area viewed by the pivot-mounted IRTs. The irrigation was applied between 16 July and 3 September for soybean and between 2 July and 5 September for maize. There were 8 irrigation events applied in soybean with a total seasonal application depth between 16 and 20 cm. There were 11 irrigation events applied in maize with a total seasonal application depth between 22 and 25 cm.

Dry Scanning using Sensors on the Pivot Lateral

The center pivot was run without water application (dry) on 16 days for data collection using the IRT and MS sensors during the 2020 growing season (table 2). The high-speed center pivot completed a revolution in about 4.1 and 5.5 h at percent timer settings of 100 and 75, respectively. The fast speed of the center pivot allowed for IRT and MS data collection across the entire field during optimal daylight hours (10:30 A.M.-4:30 P.M.). Data were collected using the dry scanning method at least once every week after the occurrence of full canopy cover. Data from the pivot-mounted sensing system could not be collected during early growth stages of the crop due to logistical reasons. In addition to dry revolutions, data from moving sensors on the pivot lateral were also collected during irrigation events.

Table 2. Days when dry scans were run for data collection in 2020.[a]

Date	Start Time	End Time	Speed %	Cloud Cover[b]
21 July	12:25 P.M.	4:34 P P.M.	100	Partly cloudy
04 Aug.	12:26 P.M.	4:31 P.M.	100	Mostly cloudy
09 Aug.	10:36 A.M.	2:43 P.M.	100	Scattered
10 Aug.	1:13 P.M.	5:20 P.M.	100	Scattered
11 Aug.	1:02 P.M.	5:08 P.M.	100	Partly cloudy
12 Aug.	10:06 A.M.	2:12 P.M.	100	Mostly cloudy
17 Aug.	9:56 A.M.	3:22 P.M.	75	Clear
18 Aug.	9:50 A.M.	3:16 P.M.	75	Mostly cloudy
19 Aug.	11:58 A.M.	5:23 P.M.	75	Partly cloudy
20 Aug.	12:16 P.M.	4:23 P.M.	100	Mostly cloudy
26 Aug.	10:29 A.M.	2:35 P.M.	100	Clear
27 Aug.	1:16 P.M.	5:22 P.M.	100	Clear
08 Sept.	10:01 A.M.	2:07 P.M.	100	Overcast
14 Sept.	10:24 A.M.	3:50 P.M.	75	Clear
15 Sept.	10:30 A.M.	3:56 P.M.	75	Scattered
16 Sept.	11:10 A.M.	4:37 P.M.	75	Partly cloudy

[a] The start and end times of each dry scan are mentioned along with the speed of the pivot in percent.

[b] The cloud cover increases in the order of clear, scattered, partly cloudy, mostly cloudy and overcast.

Data Analysis

The NDVI and SAVI data acquired during the 16 dry scans were compared among the different MS sensing systems for both maize and soybean. The red and near infrared bands of MS imagery from the UAS were used to compute NDVI and SAVI. The soil brightness correction factor for SAVI was used as 0.5 for each sensing system. For the UAS and SRS, the VIs were estimated after 21 July 2020, when the crops had reached their peak vegetative stage (100% canopy cover for maize and greater than 85% of the maximum canopy cover for soybean). For maize, there were no VI data from the UAS. The VIs were estimated throughout the growing season for the Planet sensing system. The Planet MS imagery was used with the SETMI model to compute daily VIs for both crops for the entire growing season from the respective planting date to the respective harvesting date for each crop. This was achieved using an exponential interpolation method (Campos et al., 2017) between the days with remote sensing inputs from Planet satellite (Neale et al., 2012). Therefore, the Planet sensing system had a daily estimation of VIs throughout the growing season. The NDVI and SAVI values estimated from the three sensing systems were compared from two rainfed and two irrigated plots for each crop. These plots were representative of the irrigated and rainfed plots in the field.

The crop water requirements for the irrigated plots were computed using the SETMI model. Since SETMI is a remote sensing-based model, a water balance was run individually for each pixel in the remote sensing input fed to the model. The pixel size used for the SETMI model was 3 m. For selecting a representative pixel in SETMI for comparison of the VIs, five random pixels from each selected plot were analyzed. The median VI value of these five pixels from that plot was used for the Planet system. For the SRS data within a plot, values from the same plot were analyzed, and the median value of the VI was used to represent the plot. Usually, three SRS measurements were recorded in a dry scan for each plot. Standard deviation was also computed for SRS data. For the UAS, the values of VI for pixels lying within the selected pixel for the Planet sensing system were averaged.

Further analysis was conducted on the thermal data collected on the 16 dry scan days from the different sensing systems. The IRT data for the stationary IRTs in a plot were averaged for the time period when the moving IRTs were collecting data inside that plot during a dry scan. The IRT data collected from the moving IRTs within a plot were also averaged. Statistical methods were applied to study if the correlation between stationary and moving IRTs was significant. The thermal data collected using UAS were averaged for each plot by averaging temperature values of the pixels lying within the plot (excluding the 6.1 m inner buffer around the edge of the plot).

The second comparison for thermal data was conducted between the UAS thermal imagery and the pivot-mounted IRTs in soybean. This comparison was also made on a plot scale basis, which could be considered a suitable scale for irrigation management of a field. These comparisons were completed to evaluate the sensing systems in providing canopy temperature information useful for irrigation scheduling methods.

An additional analysis was focused on studying the impact of irrigation water on the pivot-mounted IRTs. Data from a dry scan day and a wet scan day were considered for this evaluation. The data from the stationary IRTs in the field and the moving IRTs on the center pivot from one irrigated and one rainfed plot in soybean were compared. The analysis focused on the temperature gradient between stationary and pivot IRT sensors over the rainfed and irrigated plots to determine the effects of irrigation on the pivot-mounted IRTs.

Data for each analysis in the study were used from the plot after excluding a 6.1 m inner buffer (fig. 2) from all four sides of the plot. This buffer was used to ensure that there were no boundary effects from the neighboring plots with different irrigation treatments. Statistical metrics such as coefficient of determination (r^2), root mean square error (RMSE), mean absolute error (MAE), mean bias error (MBE), and regression equations, were computed for linear regression analyses on thermal data. These metrics were computed using Microsoft Excel (Microsoft Corporation, Redmond, Wash.). The method of least squares was used to select the linear regression model and compute the intercept and slope of each correlation. The RMSE, MAE and MBE were computed using the following equations:

$$\text{RMSE} = \sqrt{\frac{1}{n}\sum_{i=1}^{n}(S_i - O_i)^2} \quad (1)$$

$$MAE = \frac{1}{n}\sum_{i=1}^{n}|S_i - O_i| \quad (2)$$

$$MBE = \frac{1}{n}\sum_{i=1}^{n}(S_i - O_i) \quad (3)$$

where S_i are predicted values, O_i are observations, and n are number of observations.

Results and Discussion

Comparison of Vegetation Indices

NDVI for both crops was plotted for the different sensing systems (fig. 3). It was observed that these sensing systems were able to capture differences in NDVI between irrigated

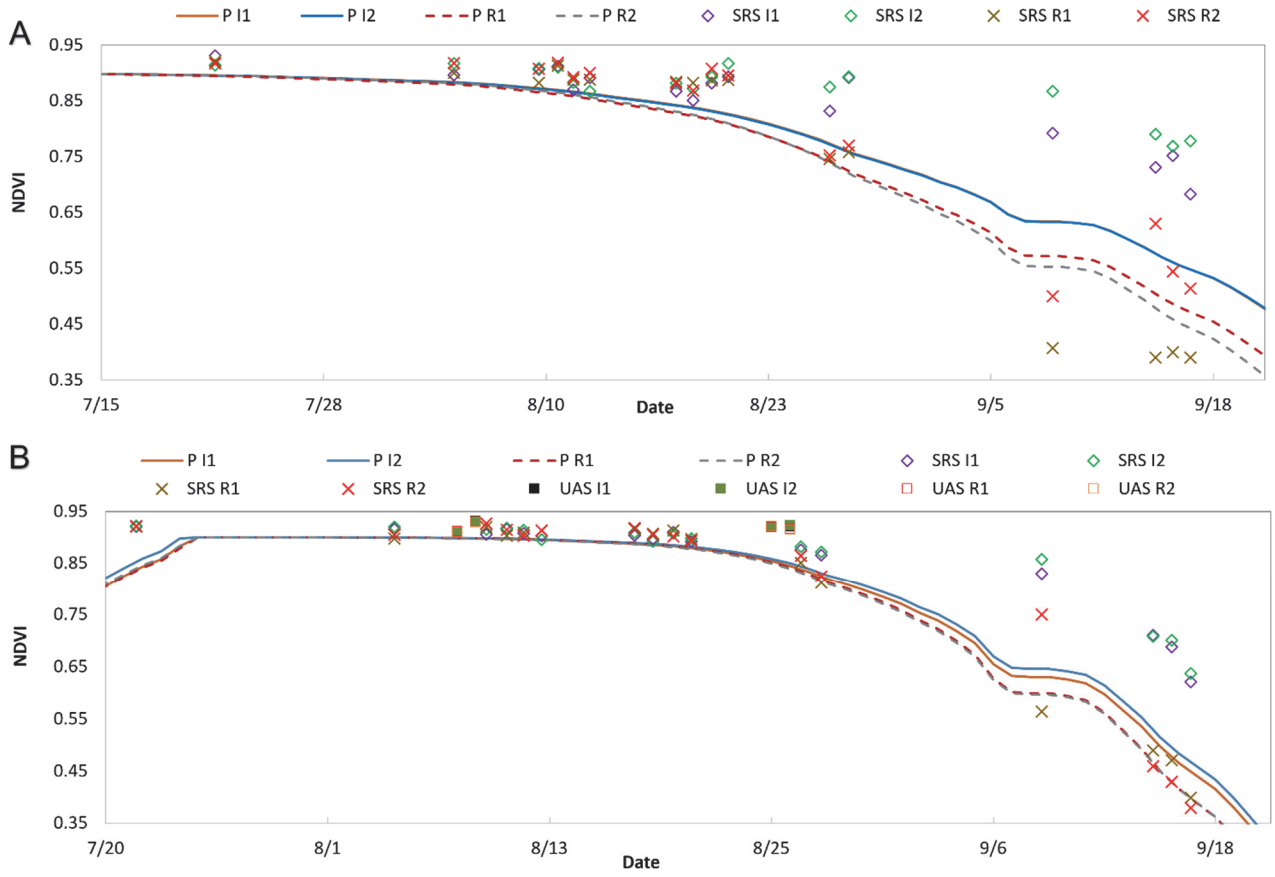

Figure 3. Normalized difference vegetation index (NDVI) computed using different sensing systems for (A) maize, and (B) soybean. The vegetation indices were computed for two irrigated and two rainfed plots for each crop. The abbreviation used to denote each data source included naming of sensing system with the irrigation type, and the plot number. The sensing systems were denoted as 'P' for Planet sensing system, 'SRS' for pivot mounted VI sensors, and 'UAS' for unmanned aircraft systems. The irrigation type was denoted using 'I' for irrigated and 'R' for rainfed followed by plot number (1 or 2).

and rainfed plots when the crops were approaching senescence. The data from all sensing systems were similar in magnitude during the peak vegetative growth for both crops. The VI data from pivot SRS were able to capture more variability among the rainfed and irrigated plots as compared with Planet when the crop approached senescence. In case of Planet data, the exponential interpolation method used for the crop VIs may have attributed to the smaller difference in crop VI values between rainfed and irrigated crop. The NDVI computed from UAS was similar in magnitude to other sensing systems for soybean during peak vegetative growth. The standard deviations of NDVI data for irrigated maize and rainfed maize were 0.06 and 0.18, respectively. The standard deviations of NDVI data for irrigated soybean and rainfed soybean were 0.09 and 0.19, respectively. The maximum value of NDVI was observed in irrigated maize (NDVI = 0.93) and minimum value was observed in rainfed maize (NDVI = 0.39).

SAVI for maize and soybean was also compared among the different data sources (fig. 4). For maize, the Planet and pivot SRS sensing systems were able to identify differences among the rainfed and irrigated crops. The standard deviations of SAVI data for irrigated maize and rainfed maize were 0.07 and 0.15, respectively. The standard deviations of SAVI data for irrigated soybean and rainfed soybean were 0.09 and 0.17, respectively. SAVI was closer in magnitude between the two data sources for rainfed as compared to the irrigated plots when the crop approached senescence. For soybean, data from UAS and Planet sensing systems were similar during the peak of the growing season. The SAVI data from pivot SRS were considerably smaller than those from Planet during the peak of canopy development and early senescence. The pivot SRS SAVI data had lower peak values during the full canopy height in soybean with an average difference of 0.1. During senescence, SAVI values from the pivot SRS and Planet were similar in magnitude. The differences in SAVI among the rainfed and irrigated plots could be identified using both pivot SRS and Planet late in the season.

The differences in VIs observed during senescence among rainfed and irrigated plots for both crops demonstrated the long-term effects of water-induced stress on physiology and canopy cover. The effects of water-induced stress resulted in lower average dry yield for rainfed maize and soybean. The average dry yield for soybean over the VI sensed area was 3.74 Mg ha^{-1} for rainfed and 4.22 Mg ha^{-1} for irrigated. The average dry yield for maize over the VI sensed area was 10.6 Mg ha^{-1} for rainfed plots and 13 Mg ha^{-1} for irrigated plots. Seasonal irrigation applied for maize was 224 mm (8.8 in.) and for soybean was 188 mm (7.4 in.). As mentioned previously, no irrigation was applied to the rainfed plots. The first irrigation was applied on 2 July for maize and 16 July for soybean. An evident difference in NDVI was noted for both crops after 26 August using the SRS mounted on the center pivot, which was more than a month after the first irrigation had occurred for both crops. This indicated

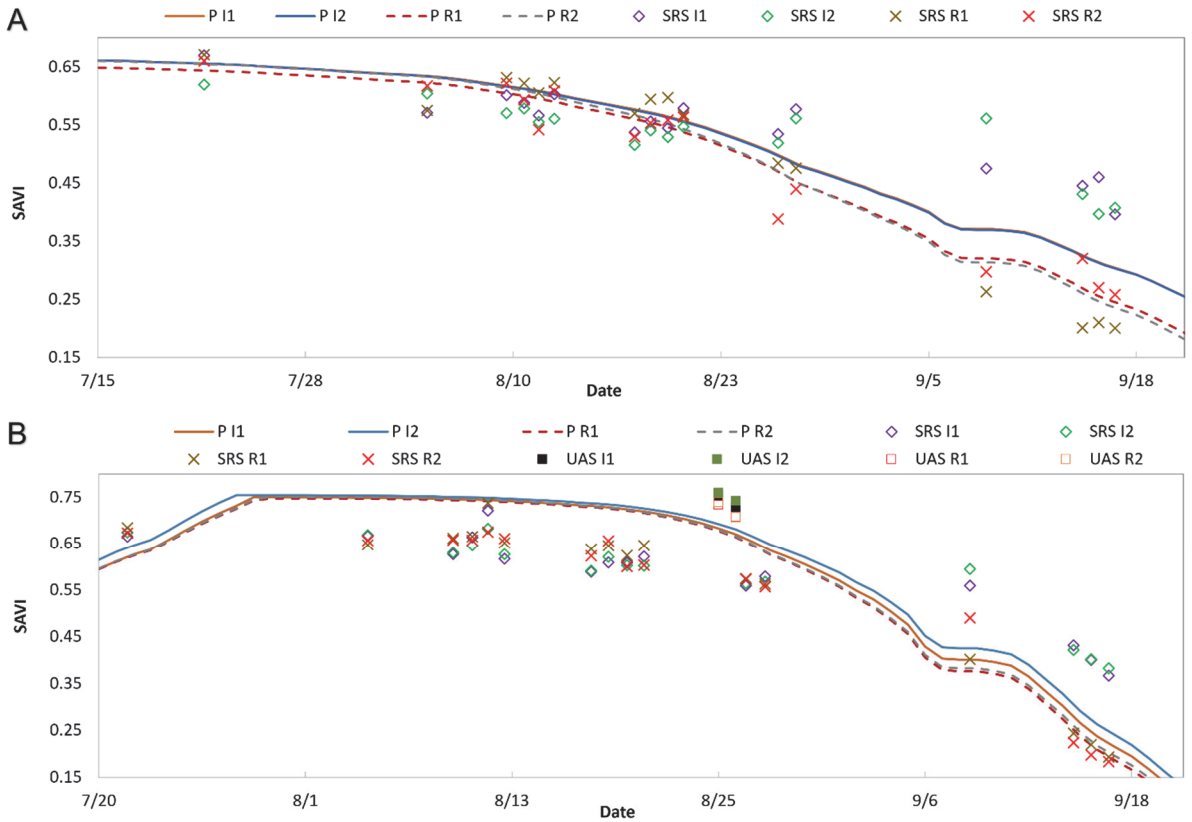

Figure 4. Soil adjusted vegetation index (SAVI) computed using different sensing systems for (A) maize, and (B) soybean. The abbreviations used to denote each data source included naming of sensing system with the irrigation type, and the plot number. The sensing systems were denoted as 'P' for Planet sensing system, 'SRS' for pivot mounted VI sensors, and 'UAS' for unmanned aircraft systems. The irrigation type was denoted using 'I' for irrigated and 'R' for rainfed followed by plot number (1 or 2).

that differences in crop physiology caused by varying levels of crop water stress among rainfed and irrigation plots were sensed by VI data with substantial time lag and may not be useful to predict real time crop water stress.

Comparison of Thermal Data

The canopy temperature data collected (21 July-16 September) using IRTs were compared among stationary and pivot sensing systems. For this comparison, the stationary IRT data were plotted on the x-axis and the data from the moving IRTs on the center pivot were plotted on the y-axis. It was found that there was a significant relationship between stationary and moving IRTs for all four crop-treatment combinations since the p-value was less than 0.01 (table 3). The intercept was not found to be significantly different from zero (p-value > 0.25) for any case at 5% level. For maize, a strong relationship was found between the two sensing systems for the irrigated plots. This relationship yielded an r^2 value of 0.99, RMSE value of 0.4°C, MAE of 0.3°C, and MBE of 0°C. These error values in the case of irrigated maize were smaller than observed by Colaizzi et al. (2019) in a maize crop (r^2 value of 0.96, RMSE value of 0.9°C, MAE of 0.7°C, and MBE of 0.5°C). They applied three deficit irrigation treatments to a maize crop and found a strong relation between data from stationary and moving IRTs (RMSE ranged from 0.65 to 1.76). The relationship between data from stationary and moving IRTs for the rainfed plots in maize yielded a r^2 value of 0.88, a higher RMSE value of 2.3°C, MAE of 1.4°C, and MBE of -1.2°C, which implied a weaker relation than found by Colaizzi et al. (2019) in irrigated maize. There were three data points for the rainfed maize case, which were the main reason for the high RMSE obtained. These three data points corresponded to 12, 20, and 26 August. If these data points were excluded, the RMSE decreased from 2.3°C to 0.7°C. The data points for irrigated maize were consistently closer to the 1:1 line as compared to the rainfed maize (fig. 5). Additionally, it was found that 81% of the data taken over rainfed maize from the pivot-mounted IRTs were within ±1.5°C of the respective data obtained from stationary sensors. For the irrigated maize, all data from moving IRTs mounted on the pivot lateral were within ±1°C of the data obtained from the respective stationary IRTs. The average ambient temperature on 8 September dropped to 8°C, due to which the canopy temperature recorded by IRTs was also low and can be seen by lower temperature values for both rainfed and irrigated plots in figure 5.

The relationship for the thermal data between the stationary and pivot-mounted moving IRTs for soybean was stronger for rainfed than for the irrigated treatment (table 3). The r^2 and RMSE obtained for rainfed soybean was 0.98 and 1.5°C, respectively as compared to 0.93°C and 2.1°C, respectively for the irrigated soybean. The MAE and MBE for rainfed soybean (1.3°C and 1.1°C, respectively) were smaller than for irrigated soybean (1.6°C and 1.4°C, respectively). Overall, a larger RMSE value was obtained for soybean as compared with maize except for three days when rainfed maize RMSE was large. For both rainfed and irrigated soybean, more than 80% of the total data obtained from pivot IRTs were within ±2.5°C of the respective data taken from the stationary IRTs. Since the correlation between stationary and moving IRT data in the case of irrigated maize is stronger than in the other three cases (table 3), it can be concluded that more accurate plant water stress was estimated using moving IRTs in irrigated maize during the period of the present study.

The pivot IRT sensor data were compared with data from the UAS thermal camera on two days during the season. The two days used for the comparison were 26 and 29 August, which were a dry scan and a wet scan day, respectively. Data

Table 3. Performance coefficients for the relation of canopy temperature between stationary and pivot infrared thermometer sensors over rainfed and irrigated plots for maize and soybean.[a]

Crop	Treatment	r^2	RMSE (°C)	MAE (°C)	MBE (°C)	Equation	P-value
Maize	Irrigated	0.99	0.4	0.3	0.0	y = 1.0267x - 0.651	2e-16
Maize	Rainfed	0.88	2.3	1.4	-1.2	y = 0.9226x + 0.8727	9.3e-8
Soybean	Irrigated	0.93	2.1	1.6	1.4	y = 1.1202x - 1.532	1.6e-9
Soybean	Rainfed	0.98	1.5	1.3	1.1	y = 1.0677x - 0.6482	9.2e-13

[a] The sample size or value of N for each case was 16. P-values were given for the correlation, which were significant for all three cases.

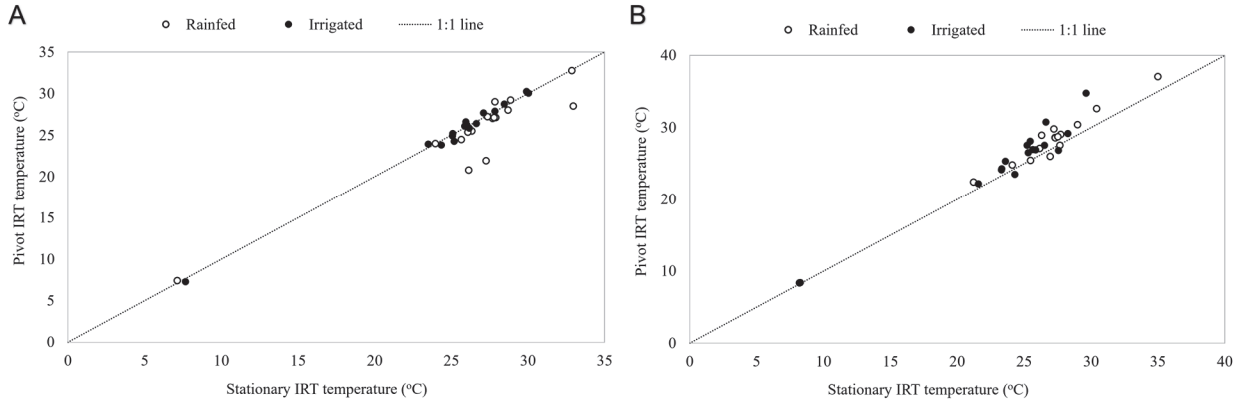

Figure 5. Comparison of canopy temperature data from infrared thermometer sensors mounted on stationary posts and the pivot lateral for (A) maize and (B) soybean. These data were collected using 16 dry scans of the pivot between 21 July-16 September.

from both sensing systems were collected during similar timestamps, which were within an hour from each other at the most. The data from both sensing systems were collected during the same time period on 29 August. About 70% of thermal data for the pivot sensing system were taken within 30 min after the UAS flight on 26 August. There were fewer data points used for the wet scan since the irrigating pivot moved slowly during the irrigation event. These two days had sunny and clear weather with reasonably consistent weather during the data collection used in the comparison. It was observed that the UAS thermal camera was reporting consistently smaller temperatures as compared with pivot IRTs for the dry scan day (fig. 6). However, the two data sources were similar in magnitude of temperature measurements when an irrigation was being applied, except for one data point. Additionally, this data point was in a rainfed plot where sprinklers were manually turned to the off position and were not irrigating. Hence, this data point could be seen as a dry scan datum and the trend was similar to the data points observed on the other dry scan day.

The UAS thermal data were within ±5°C of data from the pivot-mounted IRTs for 86% of the total measurements used in the comparison. The r^2, RMSE, MAE and MBE obtained during the dry scan day were 0.28, 3.7°C, 3.3°C, and -3.3°C respectively. The r^2, RMSE, MAE, and MBE obtained during the wet scan day were 0.26, 2.0°C, 1.4°C, and -0.6°C respectively. It was found that the UAS thermal values were consistently smaller than the pivot IRT values since the MAE and MBE were equal for the comparison using dry scan data. This result was consistent with the results found by Maguire et al. (2021).

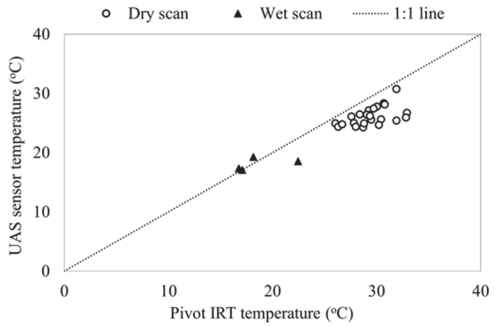

Figure 6. Relation between canopy temperature measurements from pivot IRT and UAS thermal camera on a dry scan day (26 August) and a wet scan day (29 August) from both irrigated and rainfed plots for soybean.

Impact of Irrigation on Data from Pivot-mounted Sensors

The impact of irrigation water on the canopy temperature data from the pivot-mounted sensors was determined. Data were used from the stationary IRTs and from the pivot-mounted moving IRTs over the rainfed and irrigated plots in soybean. A dry scan day (20 August) and an irrigation event (22 August) were used for this analysis. The IRT sensors over the rainfed and irrigated plots for both the stationary and pivot-mounted moving IRTs were sensing temperature from a dry canopy on the dry scan day. This could be seen in figure 7A, where IRT data from all sensing systems consistently followed a similar trend except for two timestamps (1:18 P.M. and 1:19 P.M.). During these two timestamps, a sudden increase in canopy temperature was observed for the pivot-mounted IRTs. This could be attributed to an increase in solar radiation around these two timestamps. The recorded incoming solar radiation at 1:14 P.M. was 800 W m^{-2}, which increased to a value of 826 W m^{-2} at 1:16 P.M., and then decreased to ~668 W m^{-2} at 1:24 P.M..

The IRT sensors on the pivot lateral moving over the rainfed plots were viewing a dry canopy since the sprinklers in these plots were manually turned off for the entire season. Further, the stationary IRTs in the rainfed crop was viewing a dry canopy throughout the measurement period. On the contrary, the stationary IRT in the irrigated crop viewed a dry canopy until the irrigation reached the canopy within its FOV. The stationary and moving IRTs over the rainfed crop recorded similar increases in temperature due to increases in solar radiation from 8:40 A.M.-11 A.M. (fig. 7B). Both sensing systems over the rainfed crop were quite similar in measurements. However, the stationary and pivot-mounted IRTs in the irrigated plot were inconsistent in measurements between time 8:40 A.M.-9:30 A.M. The pivot IRTs over the irrigated crop consistently recorded smaller temperature values as compared with other data sources throughout the measurement period. At around 9:30 A.M., the pivot lateral passed over the

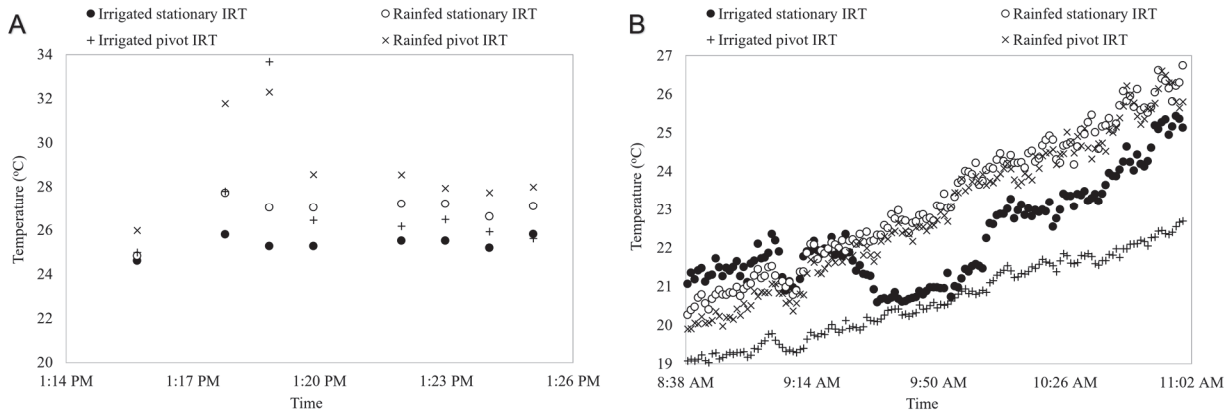

Figure 7. Canopy temperature measurements from stationary and pivot IRT sensors over rainfed and irrigated plots for (A) a dry scan day (20 August) and (B) a wet scan day (22 August). The data collected only during the time when the pivot was going over the plot with stationary sensors was used in this figure.

stationary IRT in the irrigated plot, wetting the canopy and leading to a sudden decrease in canopy temperature of 1.5°C (22°C to 20.5°C). During this period, data from the stationary and pivot-mounted IRTs in the irrigated crop were very similar, with an average difference of about 0.4°C. After the sprinkler was no longer wetting the canopy below the stationary IRT, the temperature recorded using the stationary IRT in the irrigated crop increased at a faster rate than did data from the pivot-mounted IRTs in the irrigated crop. These data indicate that the pivot-mounted IRTs were viewing a wet canopy during irrigation events, which was also visually observed in the field during catch can tests conducted on the pivot. This result was expected since the wetted radius of throw for nozzles in span 6 were in the range of 7.6 m.

Practical Considerations

Running a dry scan just before irrigating is the best time to sense stress signals from crop canopy. It was also investigated whether the canopy temperature data collected during an irrigation event could potentially inform the subsequent irrigation event. Since the temperature data from the moving IRTs mounted on the center pivot were substantially cooled by irrigation water, it is not recommended to use these data to detect crop water stress when the FOV of the IRTs is within the range of the wetted diameter of the sprinklers. The wetted radius and height of sprinklers are important considerations when designing the spacing of pivot-mounted IRTs ahead of the pivot lateral. For IRTs mounted on center pivot laterals to view a dry canopy with the sprinkler configuration used in this study, the IRTs should be mounted at least 7 m ahead of the pivot lateral such that the oblique FOV of the sensor is sensing a dry canopy. Depending on the design and materials of the IRT mounting hardware, increasing the spacing of IRTs away from the pivot lateral could add additional off-center weight that might require counterbalance weights on the other side of the lateral to maintain the proper balance. The second option to collect canopy temperature using pivot-mounted sensors over a large-scale field is to use dry scans. A third option is to use an irrigation application system that does not wet the canopy or minimally wets the canopy such as a low elevation sprinkler application (LESA) system.

The travel speed of a center pivot can be varied while running dry scans for data collection. In this study, the center pivot was run at travel time speeds of 75% and 100% for dry scan data collection. For the center pivot in this study, it was determined that the 75% speed takes about 5.5 h to complete a revolution as compared to 4 h using 100% speed. Consequently, the moving IRTs could collect about 13 data points at 75% speed and about 10 data points at 100% speed from each plot. The slower speed of the pivot could be beneficial for more representative data collection on a day with more variable weather. The slower speed during a dry scan is a good option for small sized plots since it will provide more time for the moving IRTs to collect data within a treatment plot or management zone.

The center pivot consumed about 61 Amp-hours to make a complete revolution at 100% speed. The power consumed at 480 V was about 30 kWh. Assuming the rate of electricity is 12 cents per kWh, the cost of energy used during a dry scan was about $3.60. Running a dry scan will increase the sprinkler downtime, therefore in addition to determining the optimal travel speed of the sprinkler to acquire adequate temperature data, it is necessary to determine the frequency of dry scans during the irrigation season. Downtime refers to the time when the irrigation system is not available for applying water to the field. This ultimately has a direct impact on the gross system capacity, which is the capacity of the system required to meet crop water needs. An increase in the system downtime will increase the required gross system capacity. It can be assumed that a center pivot has a downtime of 2% for maintenance and repair. The dry scan at 100% speed will increase this downtime by about 4% if a dry scan is conducted every four days (increase in downtime = 4 h/4 days). Hence, the downtime for this sprinkler system due to dry scans increases from 2% to 7%. This increase leads to an increase in gross system capacity requirement by 5% (Equation 4; Eisenhauer et al., 2021). A system that takes longer to complete a dry scan will require a greater gross system capacity. This is because of the relative increase in downtime due to slower dry scans and more reduction in system capacity. The reduced system capacity could become a problem if the crop water needs were to exceed the system capacity, specifically in times of peak water demand.

$$C_g = \frac{C_n}{\frac{E_{LQ}}{100\%}\left(1-\frac{D_t}{100\%}\right)} \quad (4)$$

where

C_g = gross system capacity,
C_n = net system capacity,
E_{LQ} = application efficiency of low quarter (%),
D_t = irrigation system downtime (%).

Further, it is important to schedule the dry scan events strategically during the week to catch the stress signal. It is advised to wait for a minimum of two days after a significant wetting event (rainfall or irrigation) to detect incipient water stress in the crop. It can be convenient to run dry scans once every week, but it may not be sufficient to detect stress during peak crop water demand. Based on the experience from this study, weekly dry scans were sufficient during most of the irrigation season for the sub-humid location. It is expected that more arid locations will require more frequent scans to detect water stress on a regular basis. The dry scans should be conducted two times in a week during the critical crop growth period. Daily monitoring of crop water stress using dry scans would be valuable and provides confidence in irrigation decision making, but may not be practical for producer fields.

Conclusions

The study compared different VIs and canopy temperature measurements estimated using different sensing systems. The thermal sensing systems used for data collection included stationary IRTs, pivot-mounted IRTs and UAS. The center pivot used in this study was a high-speed machine, capable of completing a revolution in about 4.1 h. The dry scan data from the pivot-mounted IRTs were collected

on 16 days in 2020 for both maize and soybean. The sensing systems used to compute VIs were able to capture differences between rainfed and irrigated plots when the crops were approaching senescence. The estimated VIs had a similar trend for each sensing system. The NDVI and SAVI estimated for maize using different sensing systems had similar trend and peak values among the irrigated and rainfed crop. The SAVI estimated for soybean using pivot-mounted sensors had a smaller peak value compared to that for SAVI estimated using aerial sensing systems. The comparison for canopy temperature between stationary and pivot-mounted sensors during dry scans yielded a strong correlation for a maize irrigated (r^2 = 0.99, RMSE = 0.4°C, MAE = 0.3°C) and a soybean rainfed crop (r^2 = 0.98, RMSE = 1.5°C, MAE = 1.3°C). The correlation between UAS and pivot-mounted sensors for canopy temperature was not strong with r^2 = 0.26 to 0.28. The correlation between the pivot and UAS sensing systems using the dry scan data yielded an RMSE of 3.7°C, and an MAE of 3.3°C. Canopy temperature measurements from dry scans can be used for crop water stress computations. Stationary and pivot-mounted sensors over the rainfed and irrigated plots were compared on a dry scan day and during an irrigation event. It was found that the irrigation event had a consistent cooling effect of approximately 2°C on the temperature data from the pivot-mounted sensors in the irrigated plots when irrigation was occurring from sprinklers installed at a height of 2.4 m from the ground and with sensors mounted at a distance of only 3 m forward of the pivot lateral. It was concluded that when sprinklers are installed such that the canopy is cooled by wetting within the field of view (FOV) of pivot-mounted sensors, then either the sensor mounting should be moved further from the lateral so that the FOV does not include wetted canopy, or the temperature data should only be collected when the center pivot is not irrigating. Future research could focus on using more advanced thermal imagers and multispectral cameras mounted on the pivot. These imagers could be used with machine learning and computer vision techniques to differentiate soil and canopy signal, which would be helpful early in the season or for crops with low vegetation cover.

Acknowledgements

This research was financially supported by the Irrigation Innovation Consortium, Valmont Industries, and the Robert B. Daugherty's Water for Food Global Institute at the University of Nebraska. In addition, we acknowledge support from the Eastern Nebraska Research and Extension Center and the Department of Biological Systems Engineering at the University of Nebraska-Lincoln. The authors are grateful to Alan Boldt, Jasreman Singh, Eric Wilkening, Nathan Turner, David Heeren, Keena Crone, Tyler Frederick, Keith Stewart, Nate Dorsey, and Mark Schroeder for their help in data collection, field operations and various other inputs for the research. The authors appreciate inputs from Daran Rudnick, Trenton Franz, and Jake LaRue on experimental design, center pivot system maintenance, and data analysis. Weather data were provided by the Nebraska Mesonet and the Nebraska State Climate Office through the High Plains Regional Climate Center.

References

Allen, R. G., Tasumi, M., Morse, A., Trezza, R., Wright, J. L., Bastiaanssen, W.,... Robison, C. W. (2007). Satellite-based energy balance for mapping evapotranspiration with internalized calibration (METRIC)-Applications. *J. Irrig. Drain. Eng., 133*(4), 395-406. https://doi.org/10.1061/(ASCE)0733-9437(2007)133:4(395)

Barker, J. B., Bhatti, S., Heeren, D. M., Neale, C. M. U., & Rudnick, D. R. (2019). Variable rate irrigation of maize and soybean in West-Central Nebraska under full and deficit irrigation. *Frontiers Big Data, 2*, 1-15. https://doi.org/10.3389/fdata.2019.00034

Bastiaanssen, W. G. M., Menenti, M., Feddes, R. A., & Holtslag, A. A. M. (1998). A remote sensing surface energy balance algorithm for land (SEBAL). *J. Hydrol., 212-213*, 198-212. https://doi.org/10.1016/S0022-1694(98)00253-4

Bhatti, S., Heeren, D. M., Barker, J. B., Neale, C. M. U., Woldt, W. E., Maguire, M. S., & Rudnick, D. R. (2020). Site-specific irrigation management in a sub-humid climate using a spatial evapotranspiration model with satellite and airborne imagery. *Agric. Water Manag., 230*, 105950. https://doi.org/10.1016/j.agwat.2019.105950

Campos, I., Neale, C. M. U., Calera, A., Balbontin, C., & Gonzalez-Piqueras, J. (2010). Assessing satellite-based basal crop coefficients for irrigated grapes (Vitis vinifera L.). *Agric. Water Manag., 98*(1), 45-54. https://doi.org/10.1016/j.agwat.2010.07.011

Campos, I., Neale, C. M. U., Suyker, A. E., Arkebauer, T. J., & Goncalves, I. Z. (2017). Reflectance-based crop coefficients REDUX: For operational evapotranspiration estimates in the age of high producing hybrid varieties. *Agric. Water Manag., 187*, 140-153. https://doi.org/10.1016/j.agwat.2017.03.022

Cohen, Y., Alchanatis, V., Sela, E., Saranga, Y., Cohen, S., Meron, M.,... Brikman, R. (2015). Crop water status estimation using thermography: Multi-year model development using ground-based thermal images. *Precis. Agric., 16*(3), 311-329. https://doi.org/10.1007/s11119-014-9378-1

Colaizzi, P. D., O'Shaughnessy, S. A., & Evett, S. R. (2018). Calibration and tests of commercial wireless infrared thermometers. *Appl. Eng. Agric., 34*(4), 647-658. https://doi.org/10.13031/aea.12577

Colaizzi, P. D., O'Shaughnessy, S. A., Evett, S. R., & Andrade, M. A. (2019). Comparison of stationary and moving infrared thermometer measurements aboard a center pivot. *Appl. Eng. Agric., 35*(6), 853-866. https://doi.org/10.13031/aea.13443

Daccache, A., Knox, J. W., Weatherhead, E. K., Daneshkhah, A., & Hess, T. M. (2015). Implementing precision irrigation in a humid climate: Recent experiences and on-going challenges. *Agric. Water Manag., 147*, 135-143. https://doi.org/10.1016/j.agwat.2014.05.018

DeJonge, K. C., Taghvaeian, S., Trout, T. J., & Comas, L. H. (2015). Comparison of canopy temperature-based water stress indices for maize. *Agric. Water Manag., 156*, 51-62. https://doi.org/10.1016/j.agwat.2015.03.023

Eisenhauer, D. E., Martin, D. L., Heeren, D. M., & Hoffman, G. J. (2021). Irrigation Systems Management. *ASABE.* https://doi.org/10.13031/ISM.2021

Evans, R. G., LaRue, J., Stone, K. C., & King, B. A. (2013). Adoption of site-specific variable rate sprinkler irrigation systems. *Irrig. Sci., 31*(4), 871-887. https://doi.org/10.1007/s00271-012-0365-x

Evett, S. R., Howell, T. A., Schneider, A. D., Upchurch, D. R., & Wanjura, D. F. (1996). Canopy temperature based automatic irrigation control. In C. R. Camp, E. J. Sadler, & R. E. Yoder (Ed.), *Proc. Int. Conf. Evapotranspiration and Irrigation Scheduling*, (pp. 207-213).

Evett, S. R., O'Shaughnessy, S. A., Andrade, M. A., Colaizzi, P. D., Schwartz, R. C., Schomberg, H. S.,... Sui, R. (2020). Theory and development of a VRI decision support system: The USDA-ARS ISSCADA approach. *Trans. ASABE, 63*(5), 1507-1519. https://doi.org/10.13031/trans.13922

Geli, H. M. E., & Neale, C. M. U. (2012). Spatial evapotranspiration modelling interface (SETMI). *Proc. Remote Sensing and Hydrology Symp.*, (pp. 171-174).

Higgins, C. W., Kelley, J., Barr, C., & Hillyer, C. (2016). Determining the minimum management scale of a commercial variable-rate irrigation system. *Trans. ASABE, 59*(6), 1671-1680. https://doi.org/10.13031/trans.59.11767

Huete, A. R. (1988). A soil-adjusted vegetation index (SAVI). *Remote Sens. Environ., 25*(3), 295-309. https://doi.org/10.1016/0034-4257(88)90106-X

Kashyap, S. P. (2021). High-frequency unmanned aircraft flights for crop canopy imaging during diurnal moisture stress. Lincoln: University of Nebraska-Lincoln.

Kim, D.-W., Yun, H. S., Jeong, S.-J., Kwon, Y.-S., Kim, S.-G., Lee, W. S., & Kim, H.-J. (2018). Modeling and testing of growth status for Chinese cabbage and white radish with UAV-based RGB imagery. *Remote Sensing, 10*(4), 563. https://doi.org/10.3390/rs10040563

Maguire, M. S., Neale, C. M. U., & Woldt, W. E. (2021). Improving accuracy of unmanned aerial system thermal infrared remote sensing for use in energy balance models in agriculture applications. *Remote Sensing, 13*(9), 1635. https://doi.org/10.3390/rs13091635

Miller, K. A., Luck, J. D., Heeren, D. M., Lo, T., Martin, D. L., & Barker, J. B. (2018). A geospatial variable rate irrigation control scenario evaluation methodology based on mining root zone available water capacity. *Precis. Agric., 19*(4), 666-683. https://doi.org/10.1007/s11119-017-9548-z

Neale, C. M. U., Geli, H. M. E., Kustas, W. P., Alfieri, J. G., Gowda, P. H., Evett, S. R.,... Howell, T. A. (2012). Soil water content estimation using a remote sensing based hybrid evapotranspiration modeling approach. *Adv. Water Resour., 50*, 152-161. https://doi.org/10.1016/j.advwatres.2012.10.008

Ohana-Levi, N., Knipper, K., Kustas, W. P., Anderson, M. C., Netzer, Y., Gao, F.,... Karnieli, A. (2020). Using satellite thermal-based evapotranspiration time series for defining management zones and spatial association to local attributes in a vineyard. *Remote Sensing, 12*(15), 2436. https://doi.org/10.3390/rs12152436

O'Shaughnessy, S. A., & Evett, S. R. (2010). Developing wireless sensor networks for monitoring crop canopy temperature using a moving sprinkler system as a platform. *Appl. Eng. Agric., 26*(2), 331-341. https://doi.org/10.13031/2013.29534

O'Shaughnessy, S. A., Evett, S. R., Andrade, A., Workneh, F., Price, J. A., & Rush, C. M. (2016). Site-specific variable-rate irrigation as a means to enhance water use efficiency. *Trans. ASABE, 59*(1), 239-249. https://doi.org/10.13031/trans.59.11165

O'Shaughnessy, S. A., Evett, S. R., Colaizzi, P. D., & Howell, T. A. (2013). Wireless sensor network effectively controls center pivot irrigation of sorghum. *Appl. Eng. Agric., 29*(6), 853-864. https://doi.org/10.13031/aea.29.9921

Osroosh, Y., Peters, R. T., Campbell, C. S., & Zhang, Q. (2016). Comparison of irrigation automation algorithms for drip-irrigated apple trees. *Comput. Electron. Agric., 128*, 87-99. https://doi.org/10.1016/j.compag.2016.08.013

Quebrajo, L., Perez-Ruiz, M., Perez-Urrestarazu, L., Martinez, G., & Egea, G. (2018). Linking thermal imaging and soil remote sensing to enhance irrigation management of sugar beet. *Biosyst. Eng., 165*, 77-87. https://doi.org/10.1016/j.biosystemseng.2017.08.013

Rouse, J. W., Hass, R. H., Schell, J. A., & Deering, D. W. (1973). Monitoring vegetation systems in the Great Plains with ERTS. *Proc. NASA ERTS Symp.*, (pp. 309-313).

Soil Survey Staff, 2018. Web Soil Survey. U.S. Department of Agriculture Natural Resources Conversation Service. Accessed from https://websoilsurvey.sc.egov.usda.gov/App/WebSoilSurvey.aspx

Sui, R., O'Shaughnessy, S. A., Evett, S. R., Andrade-Rodriguez, A., & Baggard, J. (2020). Evaluation of a decision support system for variable-rate irrigation in a humid region. *Trans. ASABE, 63*(5), 1207-1215. https://doi.org/10.13031/trans.13904

Taghvaeian, S., Andales, A. A., Allen, L. N., Kisekka, I., O'Shaughnessy, S. A., Porter, D. O.,... Aguilar, J. (2020). Irrigation scheduling for agriculture in the United States: The progress made and the path forward. *Trans. ASABE, 63*(5), 1603-1618. https://doi.org/10.13031/trans.14110

Zhang, J., Guan, K., Peng, B., Pan, M., Zhou, W., Jiang, C.,... Miner, G. L. (2021). Sustainable irrigation based on co-regulation of soil water supply and atmospheric evaporative demand. *Nat. Commun., 12*(1), 1-10. https://doi.org/10.1038/s41467-021-25254-7

Zhang, N., Wang, M., & Wang, N. (2002). Precision agriculture: A worldwide overview. *Comput. Electron. Agric., 36*(2), 113-132. https://doi.org/10.1016/S0168-1699(02)00096-0

Zhang, Y., Han, W., Niu, X., & Li, G. (2019). Maize crop coefficient estimated from UAV-measured multispectral vegetation indices. *Sensors, 19*(23), 5250. https://doi.org/10.3390/s19235250

Zipper, S. C., & Loheide II, S. P. (2014). Using evapotranspiration to assess drought sensitivity on a subfield scale with HRMET, a high resolution surface energy balance model. *Agric. For. Meteorol., 197*, 91-102. https://doi.org/10.1016/j.agrformet.2014.06.009